Crystallographic and magnetic properties of the mixed-valence oxides $CaRu_{1-x}Mn_xO_3$

T. Taniguchi,[1] S. Mizusaki,[1] N. Okada,[1] Y. Nagata,[1,*] S. H. Lai,[2] M. D. Lan,[2] N. Hiraoka,[3] M. Itou,[4] Y. Sakurai,[4] T. C. Ozawa,[5] Y. Noro,[6] and H. Samata[7]

[1]*College of Science and Engineering, Aoyama Gakuin University, Fuchinobe, Sagamihara, Kanagawa 157-8572, Japan*

[2]*Department of Physics, National Chung Hsing University, Taichung, 402 Taiwan, Republic of China*

[3]*Taiwan National Synchrotron Radiation Research Center, Hsin-Ann Road, Hsinchu Science Park, Hsinchu, 30076 Taiwan, Republic of China*

[4]*Japan Synchrotoron Radiation Research Institute (JASRI/SPring-8), Sayo, Hyogo 679-5198, Japan*

[5]*Nanoscale Materials Center, National Institute for Materials Science, Namiki, Tsukuba, Ibaraki 305-0044, Japan*

[6]*Kawazoe Frontier Technologies, Co. Ltd., Kuden, Sakae, Yokohama, Kanagawa 931-113, Japan*

[7]*Faculty of Maritime Sciences, Kobe University, Fukaeminami, Higashinada, Kobe, Hyogo 658-0022, Japan*

(Received 13 November 2006; revised manuscript received 1 October 2007; published 3 January 2008)

The crystallographic and magnetic properties of $CaRu_{1-x}Mn_xO_3$ ($0 \leq x \leq 1.0$) were investigated in detail by x-ray powder diffraction, magnetization, and magnetic Compton scattering measurements. The lattice parameters show considerable deviation from Vegard's law. Ferromagnetism appears at a relatively large Mn concentration ($x \geq 0.2$), and the magnetization and the Curie temperature have a maximum at a Mn content near $x=0.7$. The magnetic Compton scattering measurement revealed that Mn makes a dominant contribution to the magnetization and the Mn moment is antiparallel to the Ru moment, which is induced by Mn doping. The anomalous change in the unit cell volume and the occurrence of ferromagnetism were discussed on the basis of the mixed-valence model of Mn^{3+}, Mn^{4+}, Ru^{4+}, and Ru^{5+} ions. The Mn-composition dependence of the spontaneous magnetization was explained semiquantitatively assuming (1) ferromagnetic coupling between Mn^{3+} and Mn^{4+} ions, (2) antiferromagnetic coupling between Ru^{5+} and Mn ions, and (3) the theoretical spin moments of Mn^{3+}, Mn^{4+}, and Ru^{5+}. The ferromagnetic interaction between Mn^{3+} and Mn^{4+} ions seems to make a dominant contribution to the Curie temperature. The $CaRu_{1-x}Mn_xO_3$ system is considered to be a ferrimagnet induced through competition between the ferromagnetic interaction between Mn ions and the antiferromagnetic interaction between Ru^{5+} and Mn ions.

DOI: 10.1103/PhysRevB.77.014406 PACS number(s): 75.47.Lx, 75.50.Gg, 75.30.−m, 75.25.+z

I. INTRODUCTION

Ruthenium oxides show interesting magnetic and electric properties due to the large spatial extent of the 4*d* wave function and the relatively strong electron correlation of 4*d* electrons. For example, RuO_2 is a metallic substance with Pauli paramagnetism, and Sr_2RuO_4 is a superconductor with T_C at 0.93 K.[1] Among ruthenium oxides, $SrRuO_3$ and $CaRuO_3$ are well-known ruthenates that have been studied for four decades. Although $SrRuO_3$ is known as a ferromagnet with the Curie temperature T_C at 165 K, the magnetism of isomorphic $CaRuO_3$ remains uncertain. The magnetic moment of $CaRuO_3$ cannot be observed in neutron diffraction and Mössbauer measurements at low temperature in spite of the antiferromagnetic behavior at high temperatures. The Curie constant corresponds to $S=1$, and the Weiss temperature Θ is negative (−140 K).[2,3] Furthermore, no magnetic order was observed in our muon spin rotation measurement at temperatures down to 0.3 K. Therefore, $CaRuO_3$ is considered to be the most suitable substance for understanding the mechanism of the occurrence of ferromagnetism. Within the framework of the self-consistent renormalization spin fluctuation theory, Kiyama *et al.* suggested that $SrRuO_3$ falls under the category of itinerant ferromagnetism and $CaRuO_3$ is a paramagnet with a strong electron correlation that is on the verge of magnetic ordering.[4]

Cao *et al.* reported that $CaRuO_3$ readily evolves into a magnetically ordered phase when Sn is slightly doped.[5] Furthermore, it has been reported that ferromagnetism occurred by the substitution of various magnetic and nonmagnetic ions, such as Ti, Mn, Fe, Ni, and Rh, into the Ru site of $CaRuO_3$.[6,7] In particular, He and Cava referred to this phenomenon as "disorder-induced ferromagnetism" and considered it to be a phenomenon that is specific to $CaRuO_3$ with a strong electron correlation. Among these doped $CaRuO_3$, the $CaRu_{1-x}Mn_xO_3$ system is particularly interesting because of its relatively large magnetic moment and higher T_C than that of the ferromagnetic $SrRuO_3$. Previously, the magnetic and transport properties of the $CaMn_{1-x}Ru_xO_3$ system were studied by Maignan and co-workers, and its ferromagnetism was explained from the viewpoint of the double exchange interaction between Mn^{4+} and Mn^{3+} ions.[8–10] However, no quantitative explanation has been given for the Mn-composition dependence of the occurrence of ferromagnetism because the system was considered to be highly inhomogeneous.

In the present study, we prepared high-quality polycrystalline specimens of $CaRu_{1-x}Mn_xO_3$ and investigated their crystallographic and magnetic properties in detail. The direction of the Mn and Ru spin moments was confirmed by a magnetic Compton scattering experiment, and the origin of the ferromagnetism and the possible magnetic structure were discussed.

II. EXPERIMENT

Polycrystalline specimens of $CaRu_{1-x}Mn_xO_3$ ($0 \leq x \leq 1.0$) were prepared by the usual solid-state reaction

method using high-purity reagents of $CaCO_3$ (99.9%), Ru metal (99.9%), and Mn_2O_3 (99.9%). A stoichiometric amount of the reagents was mixed in an agate mortar, and the mixture was calcined at 1000 °C for 6 h. After the mixture was reground and pelletized under the pressure of 100 kg/cm^2, sintering was performed at 1200 °C for 48 h. The mixing and sintering were repeated several times so as to obtain homogenous specimens. The sintered pellet was annealed at 480 °C for 2 days in an oxygen atmosphere.

The chemical composition and homogeneity of the specimen were characterized by electron-probe microanalysis using wavelength-dispersive spectrometers. The crystal structure was characterized by x-ray powder diffraction using Cu $K\alpha$ radiation and subsequent refinement of the diffraction data using the Rietveld method. The electronic states of Mn and Ru ions were examined by x-ray photoelectron spectroscopy (XPS) using a photon energy of 1253.6 eV (Mg $K\alpha$). The magnetic property was characterized using a superconducting quantum interference device magnetometer at temperatures between 2 and 300 K under an applied magnetic field up to 70 kOe. The magnetic Compton profile was measured at the beamline BL08W of SPring-8 after cooling the specimen down to 10 K under an applied field of 25 kOe. The details of the experiment are described in Refs. 11–15.

III. RESULTS AND DISCUSSION

A. Crystallographic properties and electronic states of Mn and Ru

All the specimens were single phase, and all the diffraction data were refined well assuming an orthorhombic $GdFeO_3$-type structure of the space group *Pnma*. In the entire composition range, specimens retained the $GdFeO_3$-type structure, and no structural change was observed. Figures 1(a) and 1(b) show the Mn-content dependence of the refined orthorhombic lattice parameters and the unit cell volume. All the lattice parameters and the unit cell volume decreased as the Mn content increased. When Ru^{4+} (0.062 nm) in $CaRuO_3$ is replaced by Mn^{4+} (0.053 nm), the lattice parameters are expected to decrease linearly following Vegard's law. However, the experimental data deviated considerably from the linearity. This indicates that some other ions with larger ionic radii and valence than those of Mn^{4+} exist in the system. Through their studies on $CaMn_{1-x}Ru_xO_3$, Maignan and coworkers suggested that Mn doping increases the oxidation state of Ru to 5+, and Mn^{3+} is introduced simultaneously to compensate for the charge unbalance.[8–10] Our neutron diffraction and Mössbauer measurements for $CaRu_{0.85}Fe_{0.15}O_3$ revealed that there is no oxygen vacancy and that Fe exists as a trivalent ion.[11,12] In this case, Ru must exist as a Ru^{5+} ion for charge compensation. Moreover, the magnetic Compton scattering measurement for $CaRu_{1-x}Ti_xO_3$ showed the existence of Ti^{3+} and Ru^{5+} ions.[13] The coexistence of trivalent 3*d* transition metal (M^{3+}) and Ru^{5+} ions seems to be a common phenomenon in the $CaRu_{1-x}M_xO_3$ system. Therefore, it is plausible expectation that some part of the doped Mn has the 3+ oxidation state rather than 4+. The average ionic radius of the Mn^{3+}-Ru^{5+} pair is estimated to be 0.0605 nm using the ionic radii reported in Ref. 14. This is larger than the radius (0.058 nm) of Mn^{4+} ion. When a Mn ion is doped as a trivalent ion along with a Ru^{5+} ion, the reduction in the lattice parameters must be smaller than that expected for simple Mn^{4+} doping. This must be the reason that the lattice parameters deviate from Vegard's law.

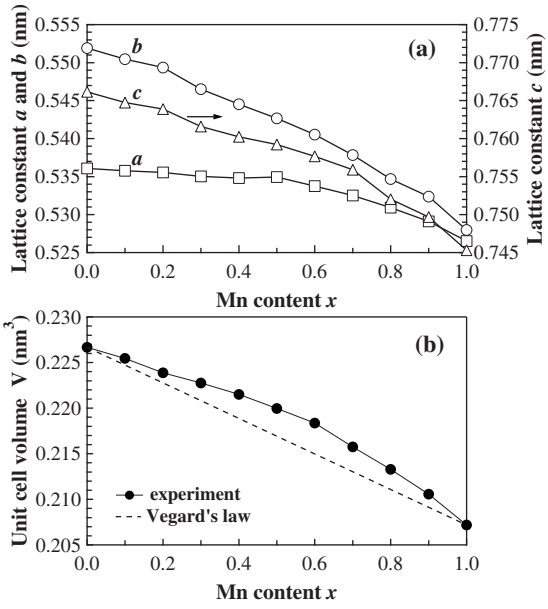

FIG. 1. The Mn-content dependence of (a) the refined orthorhombic lattice parameters and (b) the unit cell volume for $CaRu_{1-x}Mn_xO_3$.

Figure 2 shows the XPS spectra of the Mn $2p_{3/2}$ and Ru $3p_{3/2}$ core levels for $CaRu_{1-x}Mn_xO_3$ with various Mn contents. Mn $2p_{3/2}$ peaks are displayed alongside those of Mn_2O_3. The peak positions were determined by fitting the theoretical profiles to the data. The peaks of Mn and Ru could not be separated to the peaks of Mn^{3+}, Mn^{4+}, Ru^{4+}, and Ru^{5+} ions. However, the binding energy of the Mn $2p_{3/2}$ core

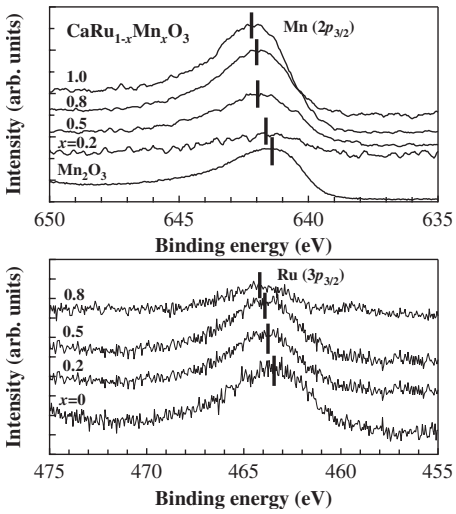

FIG. 2. The XPS spectra of Mn $2p_{3/2}$ and Ru $3p_{3/2}$ core levels for $CaRu_{1-x}Mn_xO_3$ with various Mn contents. Bars indicate the peak position obtained by the fitting.

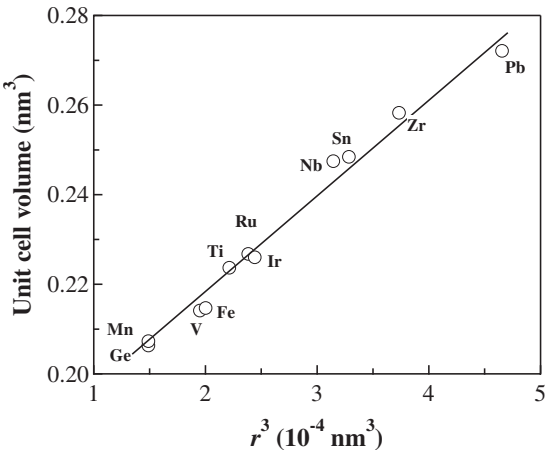

FIG. 3. The unit cell volume of the isomorphic CaMO$_3$ (M =Mn,V,Fe,Ti,Ru,Ir,Nb,Sn,Zr,Pd) as a function of the cube of the ionic radii of M ions.

level in CaRu$_{1-x}$Mn$_x$O$_3$ is larger than that of Mn^{3+} in Mn_2O_3 but smaller than that of Mn^{4+} in $CaMnO_3$, suggesting that Mn has an average ionic valence between 3+ and 4+. When the Mn content increases, the Mn $2p_{3/2}$ peak shifts to higher energies and approaches the binding energy of Mn in $CaMnO_3$. On the other hand, the Ru $3p_{3/2}$ peak also shifts to higher energies as the Mn content increases, suggesting the generation of Ru^{5+} ions. These results suggest the coexistence of Mn^{3+}, Mn^{4+}, Ru^{4+}, and Ru^{5+} ions in the CaRu$_{1-x}$Mn$_x$O$_3$ system.

Figure 3 shows the unit cell volume of isomorphic CaMO$_3$ (M=Ti,V,Mn,Fe,Ge,Zr,Nb,Ru,Sn,Ir,Pb) as a function of the cube of the average ionic radius of the transition metal ions.[14] It is seen that the unit cell volume V is proportional to the cube of the average ionic radius r_m of the transition metal ions. This suggests that the average ionic radius of transition metal ions can be estimated from the unit cell volume. The relation

$$V = 224.3r_m^3 + 0.1735 \quad (1)$$

was obtained by a linear approximation. As reported above, Mn^{3+}, Mn^{4+}, Ru^{4+}, and Ru^{5+} ions seem to coexist in the CaRu$_{1-x}M_x$O$_3$ system. In this case, r_m is represented by the relation

$$r_m = r_{\mathrm{Mn3}}t + r_{\mathrm{Mn4}}(x-t) + r_{\mathrm{Ru5}}t + r_{\mathrm{Ru4}}(1-x-t), \quad (2)$$

where r_{Mn3}, r_{Mn4}, r_{Ru4}, and r_{Ru5} are the ionic radii of Mn^{3+}, Mn^{4+}, Ru^{4+}, and Ru^{5+} ions, respectively, and x and t are the Mn content and the fraction of the Mn^{3+} ion, respectively. r_m can be estimated from relation (1) using the experimentally obtained unit cell volume V, and the fraction of each ion can then be determined for specimens with various Mn compositions following relation (2) using the reported ionic radii of metal ions.[15] The estimated fractions of each ion are listed in Table I. It is evident that the concentrations of Mn^{3+} and Mn^{4+} are almost the same as long as Ru^{5+} can compensate for the charge unbalance caused by the substitution of Mn^{3+}. The coexistence of Mn^{3+} and Mn^{4+} ions will exert a considerable influence on the magnetic properties of CaRu$_{1-x}$Mn$_x$O$_3$. In the following section, the magnetic properties are discussed using the ionic fractions shown in Table I.

TABLE I. The experimental cell volume, estimated average ionic radius, calculated ionic fraction, theoretical moment, and estimated fraction of Mn^{3+}-Mn^{4+} pairs. The average ionic radii were calculated by Eq. (1) using the cell volume, and the ionic fractions were calculated by Eq. (2) using the average ionic radii. The fractions of Mn^{3+}-Mn^{4+} pairs were assumed to be equivalent to the Mn^{3+} ion fraction.

Mn content	Cell volume (nm^3)	Average ionic radius[a] (nm)	Mn^{3+} fraction	Mn^{4+} fraction	Ru^{4+} fraction	Ru^{5+} fraction	Theoretical moment[b] (μ_B/f.u.)	Fraction of Mn^{3+}-Mn^{4+} pairs
0	0.2267	0.0620	0	0	1.00	0	0	0
0.1	0.2255	0.0615	0.06	0.04	0.84	0.06	0.18	0.06
0.2	0.2239	0.0607	0.09	0.11	0.71	0.09	0.42	0.09
0.3	0.2228	0.0602	0.16	0.14	0.54	0.16	0.59	0.16
0.4	0.2215	0.0597	0.21	0.19	0.39	0.21	0.78	0.21
0.5	0.2200	0.0589	0.24	0.26	0.26	0.24	1.01	0.24
0.6	0.2184	0.0582	0.27	0.33	0.13	0.27	1.26	0.27
0.7	0.2158	0.0570	0.22	0.48	0.08	0.22	1.54	0.22
0.8	0.2133	0.0559	0.18	0.62	0.02	0.18	1.26	0.18
0.9	0.2106	0.0546	0.10	0.80	0	0.10	0.82	0.10
1.0	0.2072	0.0530	0	1.00	0	0	0	0

[a]The ionic radii of Mn^{3+}, Mn^{4+}, Ru^{4+}, and Ru^{5+} were assumed as 0.0645, 0.053, 0.062, and 0.0565 nm, respectively, following the report by Shannon (Ref. 14).

[b]Theoretical moments were calculated using the fraction of each ion assuming the spin moments of Mn^{3+}, Mn^{4+}, Ru^{4+}, and Ru^{5+} as $4\mu_B$, $3\mu_B$, $2\mu_B$, and $3\mu_B$, respectively.

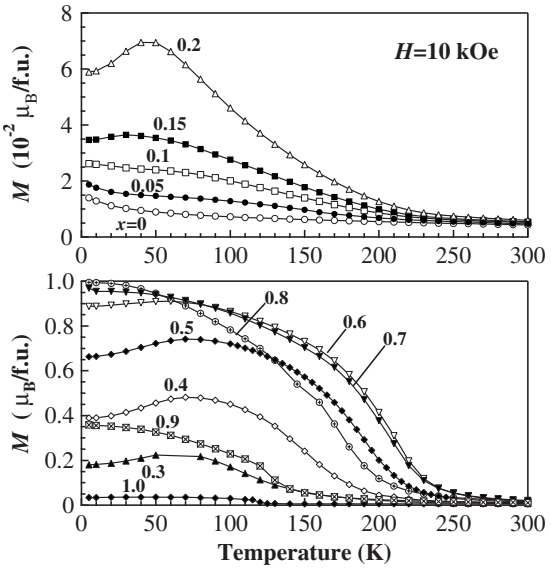

FIG. 4. The temperature dependence of the magnetization for $CaRu_{1-x}Mn_xO_3$ under an applied field of 10 kOe.

B. Magnetic properties

1. Magnetization measurements

Figure 4 shows the temperature dependence of the magnetization measured for $CaRu_{1-x}Mn_xO_3$ under an applied field of 10 kOe. The $M(T)$ curves of specimens with a Mn content of $x \geqslant 0.2$ show ferromagnetic behavior. The Mn-content dependence of T_C and the Weiss temperature Θ are shown in Fig. 5. T_C was determined as a reflection point of the $M(T)$ curve by differentiating the magnetization with respect to the temperature, and Θ was determined by fitting the Curie-Weiss formula to the $M(T)$ data. The $M(T)$ curves are consistent with those reported in former studies regarding the fact that ferromagnetism with relatively high T_C occurs by Mn doping.[7,8] It is seen that Θ changes its sign from negative to positive at about $x=0.15$. In the ferromagnetic composition range, T_C increases as the Mn content increases and has a maximum at $x=0.7$ ($T_C \sim 170$ K). This is essentially similar to the results of Maignan *et al.*[8] but differs from those of He and Cava,[7] in which the T_C was almost independent of the Mn content. This discrepancy seems to be due to the difference in the quality of specimens. In the present study,

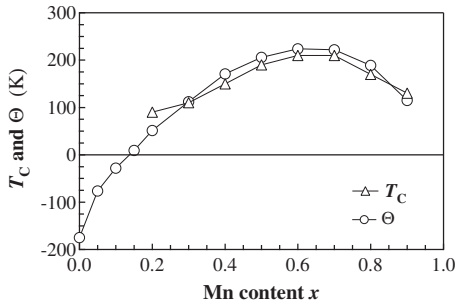

FIG. 5. The Mn-content dependence of the Curie temperature T_C and the Weiss temperature Θ for $CaRu_{1-x}Mn_xO_3$.

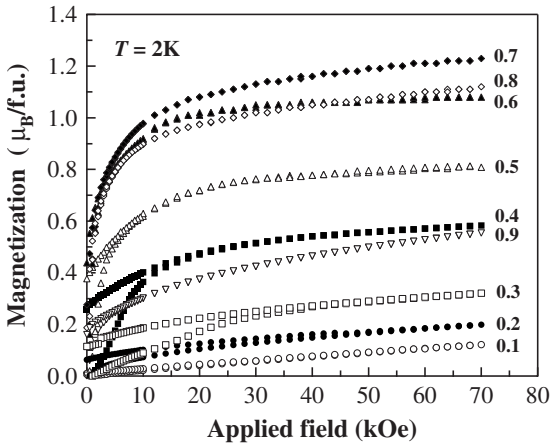

FIG. 6. The magnetic-field dependence of the magnetization for $CaRu_{1-x}Mn_xO_3$ at 2 K.

the composition dependence of the T_C was observed clearly when the specimens were prepared under a well-controlled condition.

The field dependence of the magnetization measured for $CaRu_{1-x}Mn_xO_3$ at 2 K is shown in Fig. 6. The $M(H)$ of specimens with $x \geqslant 0.1$ shows hysteresis; however, $M(H)$ of the specimens with $0.1 \leqslant x \leqslant 0.3$ shows a linear increase at higher magnetic fields and does not approach saturation even at 70 kOe. On the other hand, specimens with a Mn content of $x \geqslant 0.4$ show typical ferromagnetic behavior that tends to saturate at higher magnetic fields. These results indicate that stable ferromagnetism is established in specimens with a relatively large Mn content. Figure 7 shows the Mn-content dependence of the magnetic moment determined at 70 kOe and the moment determined by extrapolating the $M(H^{-1})$ plot to $H^{-1}=0$. The magnetic moment increases remarkably at about $x=0.3$ and shows a sharp decrease as the Mn content increases after reaching the maximum at $x=0.7$. This behavior differs considerably from that of $CaRu_{1-x}Fe_xO_3$.

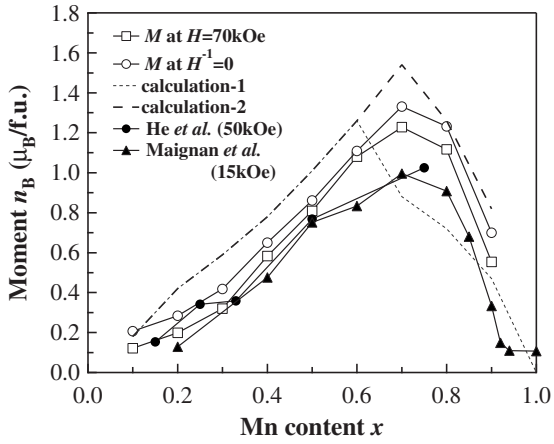

FIG. 7. The Mn-content dependence of the magnetic moment determined at 70 kOe, the moment determined by extrapolating the $M(H^{-1})$ plot to $H^{-1}=0$, and the moment estimated by assuming the mixed valence model. The data reported by He and Cava (Ref. 7) and Maignan *et al.* (Ref. 8) are also shown for comparison.

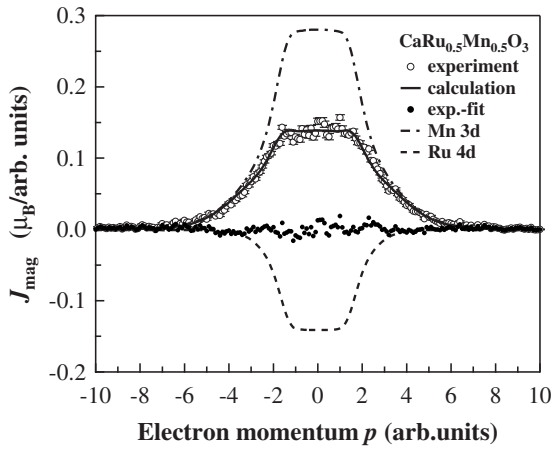

FIG. 8. The experimental magnetic Compton profile (open circle) of $CaRu_{0.5}Mn_{0.5}O_3$ at 10 K under a field of ±2.5 T and the profile (solid line) simulated on the basis of the ferrimagnetic model. The one-dot chain line and the broken line are the calculated RHF Compton profiles for Mn 3*d* and Ru 4*d* electrons, respectively.

It is well known that in the $CaRu_{1-x}Fe_xO_3$ system ferromagnetism appears for a very small Fe doping ($x \ll 0.1$) and the magnetic moment has a maximum at $x=0.15$. Our magnetic Compton scattering experiment revealed that the ratio of the Fe spin moment to the Ru spin moment is 0.5 for a specimen of $x=0.15$,[16] indicating that Ru makes a dominant contribution to the magnetization of $CaRu_{1-x}Fe_xO_3$. The magnetism of $CaRu_{1-x}Fe_xO_3$ was explained by the $FeRu_6$ cluster model, in which a Fe ion induces a magnetic moment on the six nearest-neighbor Ru ions and the Fe ion couples with six surrounding Ru ions antiferromagnetically. Ferromagnetism (or ferrimagnetism) occurs when the clusters order ferromagnetically by sharing a Ru ion.[11] On the contrary, ferromagnetism appears at a relatively large Mn content in the $CaRu_{1-x}Mn_xO_3$ system. If Ru in $CaRu_{1-x}Mn_xO_3$ is in the same electronic state as that in $CaRu_{1-x}Fe_xO_3$ and the $MnRu_6$ cluster participates to the ferromagnetism, ferromagnetism will appear with very small Mn doping ($x \ll 0.1$). Therefore, another model that is different from that of Fe doping must be considered to explain the ferromagnetism of $CaRu_{1-x}Mn_xO_3$.

2. Magnetic Compton scattering measurements

Figure 8 shows the magnetic Compton scattering profile for $CaRu_{0.5}Mn_{0.5}O_3$ at 10 K under a field of 25 kOe. $J_{mag}(p_z)$ is the one-dimensional projection of the spin-polarized electron momentum density given by

$$J_{mag}(p_z) = \int\int [n\uparrow(p) - n\downarrow(p)]dp_x dp_y,$$

where $n\uparrow(p)$ and $n\downarrow(p)$ are the momentum densities of the majority and minority spin bands, respectively, and the area under $J_{mag}(p_z)$ is equal to the total spin moment per f.u.[17–20] The magnetic moment of $0.92\mu_B$/f.u. was assigned to the experimental magnetic Compton profile (MCP) in comparison with the MCP of standard Fe metal. This value is consistent with the result of the magnetization measurement, which is shown in Fig. 7. The MCP was decomposed into the Mn 3*d* and Ru 4*d* profiles by fitting the experimental profile to that obtained by an *ab initio* restricted Hartree-Fock (RHF) cluster calculation.[21,22] The calculated RHF Compton profiles for Mn 3*d* and Ru 4*d* electrons are shown in Fig. 8. The ratio of the Mn spin moment to the Ru spin moment was determined to be 2.3, and the experimental MCP could be fitted well when the magnetic moments of $1.62\mu_B$/f.u. and $-0.71\mu_B$/f.u. were assigned for the Mn 3*d* and Ru 4*d* profiles, respectively. This result indicates that the Mn spin makes a dominant contribution to the magnetization and is antiparallel to the Ru spin moment, which is induced by Mn doping.

Following the ionic fractions shown in Table I, the Mn spin moment was calculated assuming the magnetic moments of Mn^{3+} and Mn^{4+} as $4\mu_B$ and $3\mu_B$, respectively. For Mn ion in $CaRu_{0.5}Mn_{0.5}O_3$, $1.7\mu_B$/f.u. is obtained. This value is consistent with the value $1.62\mu_B$ obtained by the Compton experiment. This fact indicates that almost all Mn spin moments align ferromagnetically in this system and contradicts the opinion that this system is highly inhomogeneous.[8] On the other hand, the magnetic moment observed for Ru is quite surprising. When the magnetic moments of $2\mu_B$ and $3\mu_B$ are assigned to Ru^{4+} and Ru^{5+} ions, respectively, and a ferromagnetic coupling between Ru^{4+} and Ru^{5+} ions is assumed, $1.3\mu_B$/f.u. is obtained for the Ru ion in $CaRu_{0.5}Mn_{0.5}O_3$ using the ion fractions shown in Table I. This value is excessively large to explain the experimental value of $0.71\mu_B$/f.u. ($\sim 1.42\mu_B$/Ru). One possible model to explain the experimental result is the cluster model that was used to explain the ferromagnetism of $CaRu_{1-x}Fe_xO_3$. However, when an average magnetic moment of $1.42\mu_B$ is induced on each Ru ion of the six nearest-neighbor sites of Mn as in the case of Fe doping,[23] ferromagnetism will appear for very small Mn substitution levels lower than $x=0.1$. Contrary to this expectation, ferromagnetism appears for relatively large Mn substitutions. Therefore, there is little possibility for the cluster model to explain the occurrence of ferromagnetism in $CaRu_{1-x}Mn_xO_3$. The MCP measurement was also performed for $CaRu_{0.7}Mn_{0.3}O_3$ and $0.39\mu_B$ was assigned to Ru. This value is considerably smaller than that of Ru in the specimen of $x=0.5$. Moreover, it is clear from the results of the MCP measurements for $x=0.3$ and 0.4 that the Ru moment increases as the Mn doping proceeds. Although it is possible to consider that the induced Ru moment grows as the Mn content increases, it seems quite natural to consider that only a portion of the Ru ions contributes to the magnetization. As pointed out above, it is quite likely that Ru^{5+} is introduced along with Mn^{3+} in the $CaRu_{1-x}Mn_xO_3$ system and the Ru^{5+} fraction increases up to $x=0.6$ as the Mn content increases. The spin moment of Ru, therefore, should be attributed to the Ru^{5+} ion. For example, when the moment of $0.71\mu_B$, which was obtained for Ru in specimens of $x=0.5$, is attributed to Ru^{5+} ions, $\sim 3\mu_B$ is assigned to a Ru ion. This value is consistent with the theoretical moment of Ru^{5+} and the experimental value ($2.8\mu_B$/Ru at 10 K) obtained for Ru^{5+} in Ba_2HoRuO_6 via the neutron diffraction measurement.[24] It is surprising that Ru^{4+} makes little contribution to the magnetic moment

in the insulating phase $CaRu_{1-x}Mn_xO_3$ ($x>0.1$). Although the reason is presently unclear, it has been reported that Ir^{5+} ($5d^4$) in Ba_2HoIrO_6 makes little contribution to the magnetic moment.[24] Since Ru^{4+} has four $4d$ electrons, similar electronic state to that of Ir^{5+} may be realized for Ru^{4+} in the insulating specimens of $CaRu_{1-x}Mn_xO_3$. In this case, Ru^{4+} will makes little contribution to the magnetic moment.

3. Composition dependence of the magnetic moment

The Mn-content dependence of the magnetic moment was calculated on the basis of the ionic fraction shown in Table I and the facts revealed by the magnetic Compton scattering experiment. The calculation was performed by assuming (1) the ionic fractions shown in Table I, (2) a ferromagnetic $Mn^{3+}Mn^{4+}$ pair, (3) antiferromagnetic coupling among excess Mn^{4+} ions, (4) an antiparallel configuration of Ru^{5+} and Mn spin moments, (5) the theoretical spin moments of Mn^{3+} ($4\mu_B$), Mn^{4+} ($3\mu_B$), and Ru^{5+} ($3\mu_B$), and (6) no magnetic moment on the Ru^{4+} site. The result of the calculation is shown in Fig. 7 [calculation (1)]. The calculation result explains the experimental result for specimens with a Mn content of $x\leqslant 0.6$; however, there are considerable discrepancies between the results of the experiment and calculations for specimens with a Mn content above $x=0.6$. As shown in Table I, there are many excess Mn^{4+} ions that cannot pair with Mn^{3+} ions in these specimens. In the above calculation, it is assumed that these Mn^{4+} ions have an antiferromagnetic order [assumption (3)] and make no contribution to the magnetization. However, it is likely that, in specimens with a relatively large Mn content ($x\geqslant 0.6$), each Mn^{3+} ion might have two nearest-neighbor Mn^{4+} ions forming a ferromagnetic trio of Mn^{4+}-Mn^{3+}-Mn^{4+} via ferromagnetic interaction. In this case, Mn^{4+} with an amount that is twice as large as that of Mn^{3+} will contribute to the magnetization of $CaRu_{1-x}Mn_xO_3$. The magnetization calculated based on this model is also shown in Fig. 7 [calculation (2)]. Although the result of the calculation agrees qualitatively with the experimental results in the wide Mn composition range, the experimental values are slightly smaller than the theoretical values. It is well known that the spin direction of Mn ions is determined through the competition between the superexchange interaction and the double-exchange interaction in the perovskite-type manganites with Mn^{3+} and Mn^{4+} ions. de Gennes pointed out that the ground state with canted-spin ferromagnetism is realized in the wide composition range when the superexchange interaction surpasses the double exchange interaction, satisfying the condition $t_0<4|J|S^2$, where J, S, and t_0 are the exchange integral, spin, and coefficient of the transfer integral, respectively.[24] Therefore, as in the case of the manganites, it is likely that the canted-spin ferromagnetism is realized in the $CaRu_{1-x}Mn_xO_3$ system at very low temperature. In this case, the experimental moment obtained from the $M(H)$ would be smaller than the theoretical value that is deduced assuming the parallel spin configuration of Mn ions. The agreement between the experimental and theoretical values strongly suggests that $CaRu_{1-x}Mn_xO_3$ is a ferrimagnet that consists of the ferromagnetic coupling between Mn^{3+} and Mn^{4+} ions and the antiferromagnetic coupling between Ru^{5+} and Mn ions.

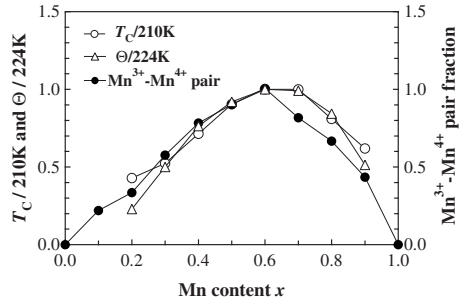

FIG. 9. The Mn-content dependence of the Curie and Weiss temperatures and the estimated fraction of Mn^{3+}-Mn^{4+} pair for $CaRu_{1-x}Mn_xO_3$. All the data have been normalized by the maximum values.

Finally, it is interesting to consider the Mn-content dependence of T_C in the $CaRu_{1-x}Mn_xO_3$ system, where the T_C is higher than those of $SrRuO_3$ (160 K) and the $CaRu_{1-x}Fe_xO_3$ system (50–90 K). The normalized Curie temperature $T_C/210$ K, the Weiss temperature $\Theta/224$ K, and the fraction of the Mn^{3+}-Mn^{4+} pair are shown in Fig. 9 as a function of the Mn content x. In this study, the fraction of the Mn^{3+}-Mn^{4+} pair is assumed to be equal to the Mn^{3+} fraction since the double-exchange interaction between Mn^{3+} and Mn^{4+} ions decreases the system energy and, therefore, a Mn^{3+} ion will adjoin a Mn^{4+} ion as much as possible forming the Mn^{3+}-Mn^{4+} pair. $T_C(x)$ and $\Theta(x)$ show similar characteristics to those of the Mn^{3+}-Mn^{4+} pair fraction below $x=0.6$, suggesting that the exchange interaction between Mn^{3+} and Mn^{4+} ions is responsible for the T_C and Θ of $CaRu_{1-x}Mn_xO_3$.

IV. CONCLUSIONS

The crystallographic and magnetic properties of the $CaRu_{1-x}Mn_xO_3$ system were investigated, and the mechanism of the occurrence of ferromagnetism was discussed. The lattice constants and the unit cell volume do not follow Vegard's law, suggesting a mixed-valence state of Mn and Ru ions. Ferromagnetism appears at a relatively large Mn concentration, and the magnetization and Curie temperature have a maximum at a Mn content near $x=0.7$. The magnetic Compton scattering measurement revealed that the magnetic moment is induced on the Ru site by Mn doping and the moment is antiparallel to the Mn spin moment, which makes a dominant contribution to the magnetization.

The Mn-composition dependence of the spontaneous magnetization and Curie temperature were consistently explained on the basis of the mixed-valence model assuming the fractions of Mn^{3+}, Mn^{4+}, Ru^{4+}, and Ru^{5+} ions, which were estimated in order to explain the Mn-content dependence of the unit cell volume. The spontaneous magnetization calculated by assuming (1) ferromagnetic coupling between Mn^{3+} and Mn^{4+}, (2) antiferromagnetic coupling between Ru^{5+} and Mn ions, and (3) the theoretical magnetic

moments of Mn^{3+} ($4\mu_B$), Mn^{4+} ($3\mu_B$), and Ru^{5+} ($3\mu_B$) satisfactorily explained the experimental result. It is likely that Ru^{4+} makes no contribution to the magnetic moment in the ferromagnetic insulating phase of $CaRu_{1-x}Mn_xO_3$. The magnetization and the Curie temperature have a maximum at a composition in which the Mn^{3+}-Mn^{4+} pair fraction is the largest, suggesting that a ferromagnetic network consisting of Mn^{3+} and Mn^{4+} ions plays a key role in the occurrence of ferromagnetism in $CaRu_{1-x}Mn_xO_3$. It is likely that a sort of ferrimagnetism is established in $CaRu_{1-x}Mn_xO_3$ at large Mn contents through competition of the ferromagnetic interaction between Mn^{3+} and Mn^{4+} ions and antiferromagnetic interaction between Ru^{5+} and Mn ions.

ACKNOWLEDGMENTS

The work conducted at Aoyama Gakuin University was supported by The 21st Century COE Program of the Ministry of Education, Culture, Sports, Science, and Technology, Japan. A part of the work performed at Aoyama Gakuin University was supported by The Private School High-Tech Research Center Program of the Ministry of Education, Culture, Sports, Science, and Technology, Japan. The work accomplished at National Chung Hsing University was supported by the National Science Council of ROC under Contract No. NSC 95-2112-M-005-010-MY3.

*Corresponding author: yunaga@ee.aoyama.ac.jp

[1] Y. Maeno, H. Hashimoto, K. Yoshida, S. Nishizaki, T. Fujita, J. Bednorz, and F. Lichtenberg, Nature (London) **372**, 532 (1994).
[2] J. M. Longo, P. M. Raccah, and J. B. Goodenough, J. Appl. Phys. **39**, 1327 (1968).
[3] T. C. Gibb, R. Greatrex, N. N. Greenwood, and P. Kaspi, J. Chem. Soc. Dalton Trans. **1973**, 253.
[4] T. Kiyama, K. Yoshimura, K. Kosuge, Y. Ikeda, and Y. Bando, Phys. Rev. B **54**, R756 (1996).
[5] G. Cao, S. McCall, J. Bolivar, M. Shepard, F. Freibert, P. Henning, J. E. Crow, and T. Yuen, Phys. Rev. B **54**, 15144 (1996).
[6] G. Cao, F. Freibert, and J. E. Crow, J. Appl. Phys. **81**, 3884 (1997).
[7] T. He and R. J. Cava, J. Phys.: Condens. Matter **13**, 8347 (2001).
[8] A. Maignan, C. Martin, M. Hervieu, and B. Raveau, Solid State Commun. **117**, 377 (2001).
[9] V. Markovich, M. Auslender, I. Fita, R. Puzniak, C. Martin, A. Wisniewski, A. Maignan, B. Raveau, and G. Gorodetsky, Phys. Rev. B **73**, 014416 (2006).
[10] A. I. Shames, E. Rozenberg, C. Martin, A. Maignan, B. Raveau, G. Andre, and G. Gorodetsky, Phys. Rev. B **70**, 134433 (2004).
[11] T. Taniguchi, S. Mizusaki, N. Okada, Y. Nagata, K. Mori, T. Wuernisha, T. Kamiyama, N. Hiraoka, M. Itou, Y. Sakurai, T. C. Ozawa, Y. Noro, and H. Samata, Phys. Rev. B **75**, 024414 (2007).
[12] A. Koriyama, M. Ishizaki, T. Taniguchi, Y. Nagata, T. Uchida, and H. Samata, J. Alloys Compd. **372**, 58 (2004).
[13] S. Mizusaki, N. Okada, T. Taniguchi, Y. Nagata, N. Hiraoka, Y. Noro, M. Ito, and Y. Sakurai, J. Magn. Magn. Mater. **310**, e325 (2007).
[14] R. D. Shannon, Acta Crystallogr., Sect. A: Cryst. Phys., Diffr., Theor. Gen. Crystallogr. **32**, 751 (1976).
[15] For Ge, S. Sasaki, C. T. Prewitt, and R. C. Liebermann, Am. Mineral. **68**, 1189 (1983); for Mn, H. Taguchi, M. Sonoda, and M. J. Nagao, J. Solid State Chem. **137**, 82 (1998); for V, J. Garcia-Jaca, J. I. R. Larramendi, M. Insausti, M. I. Arriortua, and T. Rojo, J. Mater. Chem. **5**, 1995 (1995); for Fe, T. Takeda, R. Kanno, Y. Kawamoto, M. Takano, S. Kawasaki, T. Kamiyama, and F. Izumi, Solid State Sci. **2**, 673 (2000); for Ti, A. Beran, E. Libowitzky, and T. Armbruster, Can. Mineral. **34**, 803 (1996); for Ru, M. V. Rama Rao, V. G. Sathe, D. Sornadurai, B. Panigrahi, and T. Shripathi, J. Phys. Chem. Solids **62**, 797 (2001); for Ir, F. Rodi and D. Babel, Z. Anorg. Allg. Chem. **336**, 17 (1965); for Nb, R. H. Mitchell, J. B. Choi, F. C. Hawthorne, C. A. McCammon, and P. C. Burns, Can. Mineral. **36**, 107 (1998); for Sn, M. Vallet-Regi, J. M. Gonzalez-Calbet, M. A. Alario-Franco, and A. Vegas, Acta Crystallogr., Sect. C: Cryst. Struct. Commun. **42**, 167 (1986); for Zr, I. Levin, T. G. Amos, S. M. Bell, L. Farber, T. A. Vanderah, R. S. Roth, and B. H. Toby, J. Solid State Chem. **175**, 170 (2003); for Pb, A. Yamamoto, N. R. Khasanova, F. Izumi, X. J. Wu, T. Kamiyama, S. Torii, and S. Tajima, Chem. Mater. **11**, 747 (1999).
[16] S. Mizusaki, N. Hiraoka, T. Nagao, M. Itou, Y. Sakurai, T. Taniguchi, N. Okada, Y. Nagata, T. C. Ozawa, and Y. Noro, Phys. Rev. B **74**, 052401 (2006).
[17] N. Sakai, J. Synchrotron Radiat. **5**, 937 (1998).
[18] N. Hiraoka, M. Itou, A. Deb, Y. Sakurai, Y. Kakutani, A. Koizumi, N. Sakai, S. Uzuhara, S. Miyaki, H. Koizumi, K. Makoshi, N. Kikugawa, and Y. Maeno, Phys. Rev. B **70**, 054420 (2004).
[19] A. Koizumi, S. Miyaki, Y. Kakutani, H. Koizumi, N. Hiraoka, K. Makoshi, N. Sakai, K. Hirota, and Y. Murakami, Phys. Rev. Lett. **86**, 5589 (2001).
[20] Y. Sakurai, M. Itou, J. Tamura, S. Nanao, A. Thamihavel, Y. Inada, A. Galatanu, E. Yamamoto, and Y. Onuki, J. Phys.: Condens. Matter **15**, S2183 (2003).
[21] M. W. Schmidt, K. K. Baldridge, J. A. Boatz, S. T. Elbert, M. S. Gordon, J. H. Jensen, S. Koseki, N. Matsunaga, K. A. Nguyen, S. Su, T. L. Windus, M. Dupuis, and J. A. Montgomery, Jr., J. Comput. Chem. **14**, 1347 (1993).
[22] Y. Sakurai, M. Itou, J. Tamura, S. Nanao, A. Thamihavel, Y. Inada, A. Galatanu, E. Yamamoto, and Y. Onuki, J. Phys.: Condens. Matter **15**, S2183 (2003).
[23] Y. Hinatsu, Y. Izumiyama, Y. Doi, A. Alemi, M. Wakeshima, A. Nakamura, and Y. Morii, J. Solid State Chem. **177**, 38 (2004).
[24] P. G. de Gennes, Phys. Rev. **118**, 141 (1960).